ISSN 0001-4338, Izvestiya, Atmospheric and Oceanic Physics, 2021, Vol. 57, No. 12, pp. 1783–1788. © Pleiades Publishing, Ltd., 2021.
Russian Text © The Author(s), 2015, published in Issledovanie Zemli iz Kosmosa, 2015, No. 5, pp. 9–15.

PHYSICAL FOUNDATIONS OF EARTH EXPLORATION FROM SPACE

Dielectric Model of Thawed and Frozen Organic Soil at the AMSR Radiometer Frequency

V. L. Mironov[a], L. G. Kosolapova[a], *, and I. V. Savin[a]

[a] *Kirensky Institute of Physics, Siberian Branch, Russian Academy of Sciences, Krasnoyarsk, 660036 Russia*

**e-mail: rsdvk@ksc.krasn.ru*

Received March 14, 2014; revised December 3, 2014; accepted December 25, 2014

Abstract—In this paper, we develop a simple single-frequency dielectric model of thawed and frozen arctic soil for a frequency of 6.9 GHz. The model is developed based on laboratory dielectric measurements of soil samples containing 80–90% organic matter in the range of gravimetric moisture from 0.01 to 0.942 g/g (volumetric moisture ranging from 0.007 to 0.573 cm^3/cm^3), and temperatures from +25 to –30°C in the freeze mode. A refractive mixture model is used as a regression equation for the measured values of the complex soil refractive index depending on moisture. The complex refractive indices of various soil components (mineral-organic , bound, transitional, and free water (ice for frozen soil)), as well as values for the maximum allowable content of bound and transitional water in the soil at all measured temperatures, are determined using the regression analysis. The empirical dependences of the complex refractive index of soil components and the maximal allowable contents of various types of water in soil on temperature are obtained. As a result, we developed a model that allows calculating the permittivity of thawed and frozen organic soil as a function of moisture and temperature at 6.9 GHz. The root-mean-square error was 0.20 for the real part of the complex dielectric permittivity of the soil and 0.22 for the imaginary part at the determination coefficient values of 0.999 and 0.995, respectively.

Keywords: organic soil, moisture, dielectric model, thawed and frozen soil, AMSR radiometer, 6.9 GHz

DOI: 10.1134/S0001433821120318

INTRODUCTION

The AMSR-E radiometer, which measures the brightness temperatures of the Earth's microwave radiation at 6.9, 10.65, 18.7, 23.8, 36.5, and 89.0 GHz at vertical and horizontal polarizations in a 1450 km wide band, operated onboard the Aqua satellite from May 2002 to October 2011. It was stopped due to increased rotational friction, and in December 2012, it was put back into operation at a lower rotational speed, and the information measured by it was again available to users. Furthermore, the Japanese GCOM W1 satellite with the AMSR2 radiometer was launched in May 2012 and is still operating, which makes measurements at seven frequencies (6.9, 7.3, 10.65, 18.7, 23.8, 36.5, and 89.0 GHz) (http://suzaku.eorc.jaxa.jp/GCOM_W/index.html). The lowest frequency of 6.9 GHz is most suitable for restoring the land surface moisture, as it is most sensitive to water. All algorithms for retrieving soil moisture from measurements of the ground brightness temperature use wet soils dielectric models (Mladenova et al., 2014). Recently, a dielectric model developed by V.L. Mironov et al. (Mironov and Fomin, 2009) for wet soils, which allows calculating the complex dielectric permittivity (CDP) of thawed mineral soils with different granulometric composition depending on soil moisture and temperature in the frequency range from 0.3 to 26.5 GHz, currently operates as a part of the SMOS data processing algorithm.

The soils of the circumpolar Arctic have a high content of organic matter. A significant stock of dead plant residues in the tundra is due to the slow mineralization of the litter, the poverty of the bacterial flora, and unfavorable soil temperatures. The upper organogenic horizon of the Arctic tundra contains more than 30% of organic carbon (Rozanov, 1975). The presence of organic matter has a significant effect on the dielectric properties of wet soils. Known formulas relating the permittivity of organic soils to the moisture content were developed to calibrate commercial reflectometers designed to measure the moisture content of thawed soils in the megahertz frequency range (Topp et al., 1989; Scierucha, 2000; Pumpanen and IIvesniemi, 2005). In the gigahertz frequency range, Mironov et al. (Mironov and Savin, 2010; Mironov et al., 2010) earlier developed a multifrequency (the frequency varies from 1.0 to 16.0 GHz) model of Arctic soil rich in organic matter in thawed and frozen states for temperature ranges of $-7°C \le T \le 25°C$ and $-30°C \le T \le -7°C$, respectively. In this model, the humidity dependences are described by the refractive model, the frequency dependences are described by

Table 1. Dry soil density ρ_d, g/cm^3. Gravimetric moisture relative to dry sample weight, m_g, g/g. Volumetric moisture m_v, cm^3/cm^3, relative to the volume of the dry sample

m_g	0.01	0.106	0.126	0.144	0.176	0.202	0.237	0.245	0.263	0.339	0.377	0.385	0.382	0.441	0.562	0.763	0.942
ρ_d	0.666	0.622	0.625	0.591	0.604	0.568	0.564	0.567	0.566	0.581	0.564	0.574	0.595	0.601	0.596	0.603	0.608
m_v	0.007	0.066	0.079	0.085	0.106	0.115	0.134	0.139	0.149	0.197	0.213	0.221	0.227	0.265	0.335	0.46	0.573

the Debye equations, and the temperature dependences are described by the Clausius-Mosotti and Debye equations and the equation for the temperature coefficient of ionic conductivity. As a result, it contains a high number of parameters and is not very convenient for practical use. Furthermore, in the multifrequency model (Mironov and Savin, 2010; Mironov et al., 2010), due to the chosen method of soil freezing, the soil freezing temperature was −7°C, while under natural conditions, the soil freezing temperature can vary in the range of negative temperatures ranging from tenths of degrees Celsius to several degrees.

In this paper, we propose a simpler single-frequency (6.9 GHz) temperature-dependent dielectric model for the same Arctic soil. In this case, due to the use of another technology for freezing soil samples, the developed dielectric model for frozen soil is applicable in the temperature range of $-30°C \le T \le -1°C$.

EXPERIMENTAL DATA AND A REFRACTIVE DIELECTRIC MODEL OF A MIXTURE

A soil sample (shrub tundra) taken by the staff of the University of Michigan near Lake Toolik (Alaska) during fieldwork in 2004 (De Roo et al., 2006) was chosen for dielectric measurements. The content of organic matter in this soil is 80–90%, the mineral component is dominated by calcite 60–70%, quartz 20–30%, and traces of mica, plagioclase, and kaolinite. The dielectric properties of the soil were measured in the frequency range from 1 to 16 GHz, gravimetric humidity varied from 0.01 to 0.942 g/g (the volumetric moisture varied from 0.007 to 0.573 cm^3/cm^3), and temperature varied from +25 to −30°C with steps of 5 and 2°C depending on the measured local range. The dry soil density in vivo was 0.254 g/cm^3, while the average dry soil density in vitro was 0.597 g/cm^3. The dry density of the soil varied from sample to sample since the filling density of the measuring cell depended on the soil moisture (Table 1).

The complex dielectric permittivity was measured using a Rohde & Schwarz ZVK vector network analyzer. The measurement method is described in (Mironov et al., 2010).

As in (Mironov et al., 2010), we will analyze the complex dielectric permittivity ε of soil in terms of the reduced complex refractive index (CRI):

$$(n^* - 1)/\rho_d = \left(\sqrt{\varepsilon} - 1\right)/\rho_d = (n-1)/\rho_d + i\kappa/\rho_d, \quad (1)$$

where $n = \mathrm{Re}\sqrt{\varepsilon}$ and $\kappa = \mathrm{Im}\sqrt{\varepsilon}$ are the real and imaginary parts of the CRI, respectively; and ρ_d is the density of dry soil composition, g/cm^3.

Figure 1 shows the results of measurements of the reduced complex refractive index in the temperature ranges of $-5°C \le T \le 25°C$ and $-30°C \le T \le 7°C$ for thawed and frozen soils, respectively. Together with the results of measurements of the reduced complex refractive index, Fig. 1 shows the regression lines obtained using the generalized refractive dielectric model of mixture (2) and (3) in the form given in (Mironov et al., 2010).

$$\frac{n_s - 1}{\rho_d(m_g)} = \begin{cases} \dfrac{n_m - 1}{\rho_m} + \dfrac{(n_b - 1)}{\rho_b} m_g; \quad m_g \le m_{g1n}, \\ \dfrac{n_m - 1}{\rho_m} + \dfrac{(n_b - 1)}{\rho_b} m_{g1n} + \dfrac{n_t - 1}{\rho_t}(m_g - m_{g1n}); \\ m_{g1n} \le m_g \le m_{g2n}, \\ \dfrac{n_m - 1}{\rho_m} + \dfrac{(n_b - 1)}{\rho_b} m_{g1n} + \dfrac{n_t - 1}{\rho_t}(m_{g2n} - m_{g1n}) \\ + \dfrac{n_{l,i} - 1}{\rho_{l,i}}(m_g - m_{g2n}); \quad m_g \ge m_{g2n}, \end{cases} \quad (2)$$

$$\frac{\kappa_s}{\rho_d(m_g)} = \begin{cases} \dfrac{\kappa_m}{\rho_m} + \dfrac{\kappa_b}{\rho_b} m_g; \quad m_g \le m_{g1\kappa}, \\ \dfrac{\kappa_m}{\rho_m} + \dfrac{\kappa_b}{\rho_b} m_{g1\kappa} + \dfrac{\kappa_t}{\rho_t}(m_g - m_{g1\kappa}); \\ m_{g1\kappa} \le m_g \le m_{g2\kappa}, \\ \dfrac{\kappa_m}{\rho_m} + \dfrac{\kappa_b}{\rho_b} m_{g1\kappa} + \dfrac{\kappa_t}{\rho_t}(m_{g2\kappa} - m_{g1\kappa}) \\ + \dfrac{\kappa_{l,i}}{\rho_{l,i}}(m_g - m_{g2\kappa}); \quad m_g \ge m_{g2\kappa}. \end{cases} \quad (3)$$

Subscripts s, d, m, b, t, l, and i denote wet soil, dry soil, organic-mineral soil component; bound, transitional, free (liquid) water; and ice, respectively; m_{g1n}, $m_{g1\kappa}$ and m_{g2n}, $m_{g2\kappa}$ are the values for the maximal allowable content of bound water and the total maximal allowable content of bound and transitional water that are determined from the humidity dependences of the real (m_{g1n}, m_{g2n}) and imaginary ($m_{g1\kappa}$, $m_{g2\kappa}$) parts of the reduced CRI, respectively. According to formulas (2) and (3), when calculating the real or imaginary parts of the CRI when the moisture content of the sample increases, the presence in the sample of only the bound component of soil water is taken into

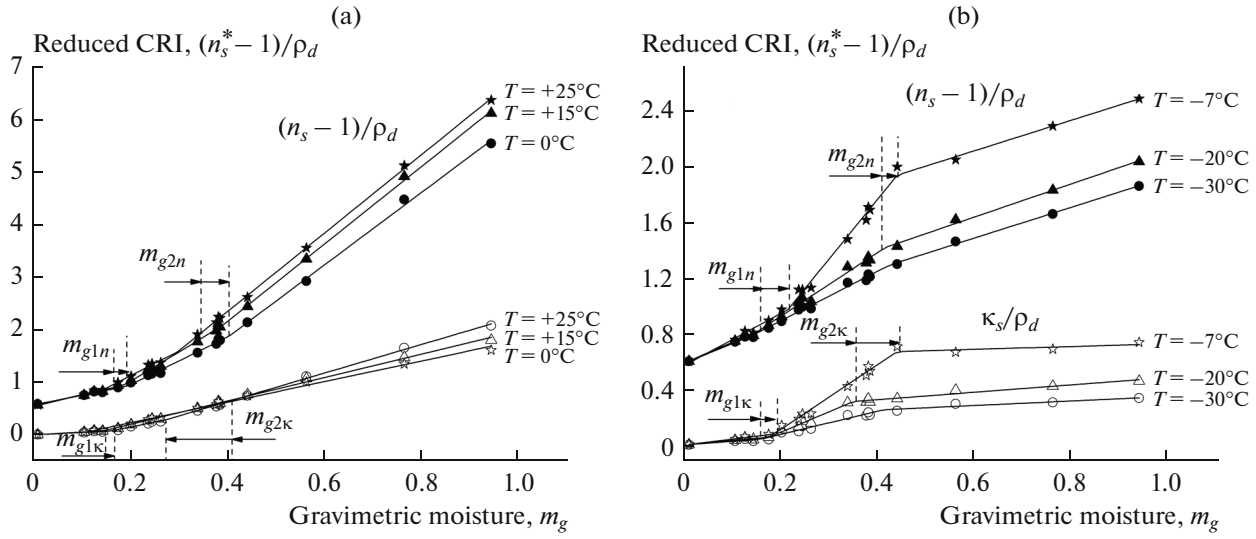

Fig. 1. Dependences of the reduced complex refractive index (CRI) of soil on the gravimetric moisture content at various temperatures T (values are shown on the graphs) at 6.9 GHz: (a) thawed soil, (b) frozen soil.

account if the inequalities of $m_g \le m_{g1n}$ or $m_g \le m_{g1\kappa}$ are satisfied, two components of soil water (bound and transitional) if the inequalities of $m_{g1n} < m_g \le m_{g2n}$ or $m_{g1\kappa} < m_g \le m_{g2\kappa}$ are satisfied, and all three (bound, transitional, and free) components of soil water if the inequalities of $m_{g2n} < m_g$ or $m_{g2\kappa} < m_g$ are satisfied.

In Fig. 1, the vertical lines show the limits of m_{g1n}, m_{g2n} and $m_{g1\kappa}$, $m_{g2\kappa}$ as a function of temperature. It turns out that the limits determined from measurements of the real (m_{g1n}, m_{g2n}) and imaginary ($m_{g1\kappa}$, $m_{g2\kappa}$) parts of the complex refractive index do not coincide. This phenomenon may be the result of the different effect of the dipole polarization and ionic conductivity of soil moisture on the values of the real and imaginary parts of the soil's CRI.

As can be seen in Fig. 1, the regression lines determined using formulas (2) and (3) describe the measured values very well. These dependences have the form of broken lines, each segment of which corresponds to the presence of a certain combination of soil water components. In this case, the change in moisture in each segment can occur only due to one component of soil water. According to formulas (2) and (3), using the regression analysis, it is possible to determine the values of the parameters $(n_q - 1)/\rho_q$ and κ_q/ρ_q corresponding to the mineral-organic component of the soil ($q = m$) and all types of water in the soil ($q = b, t, l, i$), as well as values for the maximal allowable bound water content (m_{g1n}, $m_{g1\kappa}$) and the total maximal allowable bound and transitional water content (m_{g2n}, $m_{g2\kappa}$) as a function of temperature.

Parameters m_{g1n}, m_{g2n}, $(n_m - 1)/\rho_m$, $(n_b - 1)/\rho_b$, $(n_t - 1)/\rho_t$, $(n_{l,i} - 1)/\rho_{l,i}$, $m_{g1\kappa}$, $m_{g2\kappa}$, κ_m/ρ_m, κ_b/ρ_b, κ_l/ρ_t, and $\kappa_{l,i}/\rho_{l,i}$ were determined at −5, 0, 5, 10, 15, 20, 25°C and −30, −25, −20, −15, −10, −7°C for thawed and frozen soils, respectively. After that, the obtained parameter values were approximated as a function of temperature by polynomials of the first, second, and third degrees separately for thawed and frozen soils.

(A) Thawed soil (−5°C ≤ T ≤ 25°C)

$$
\begin{gathered}
m_{g1n} = 0.214 + 2.77\times10^{-4}T \\
- 1.952\times10^{-4}T^2 + 5.111\times10^{-6}T^3; \\
m_{g2n} = 0.405 + 7.524\times10^{-4}T - 1.276\times10^{-4}T^2; \\
(n_m - 1)/\rho_m = 0.56 - 0.0017T + 3.076\times10^{-5}T^2; \\
(n_b - 1)/\rho_b = 2.067 + 0.02566T \\
- 0.0013T^2 + 3.571\times10^{-5}T^3; \\
(n_t - 1)/\rho_t \\
= 4.566 + 0.11T - 0.0012T^2 - 5.715\times10^{-5}T^3; \quad (4) \\
(n_l - 1)/\rho_l = 6.82 + 0.0648T - 0.00155T^2; \\
m_{g1\kappa} = 0.163 + 3.286\times10^{-4}T - 3.429\times10^{-4}T^2; \\
m_{g2\kappa} = 0.44; \\
\kappa_m/\rho_m = 0.00923 - 5.214\times10^{-5}T; \\
\kappa_b/\rho_b = 0.455 + 0.00664T; \\
\kappa_t/\rho_t = 2.0461 + 0.0483T - 0.00165T^2; \\
\kappa_l/\rho_l = 2.724 - 0.0503T.
\end{gathered}
$$

Formulas (1)–(4) represent a refractive model of the complex dielectric permittivity of thawed organic soil at 6.9 GHz.

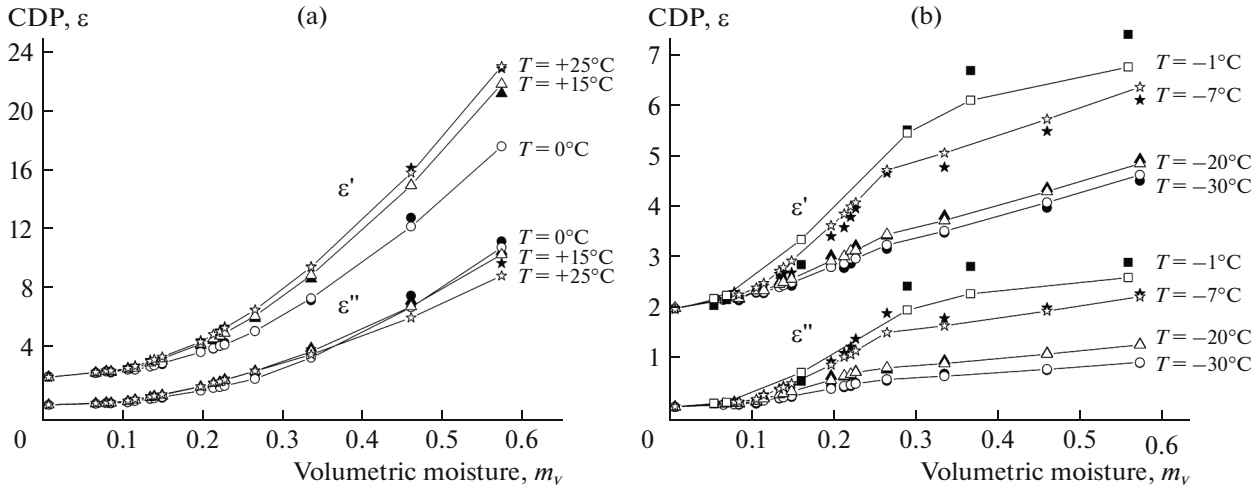

Fig. 2. Dependences of measured (filled symbols) and calculated according to the CDP model (empty symbols) soil on volumetric moisture at different temperatures, T (values are shown in the graphs) and different soil densities (values are shown in Table 1): (a) thawed soil, (b) frozen soil. The points corresponding to the calculation are connected by straight line segments.

(B) Frozen soil ($-30°C \le T \le -7°C$)

$$\begin{gathered}
m_{g1n} = 0.2 + 0.0037T + 6\times10^{-5}T^2;\\
m_{g2n} = 0.461 + 0.00244T + 4.147\times10^{-5}T^2;\\
(n_m - 1)/\rho_m = 0.5554 - 0.00365T - 8.412\times10^{-5}T^2;\\
(n_b - 1)/\rho_b = 2.208 + 0.063T + 0.00124T^2;\\
(n_t - 1)/\rho_t = 5.839 + 0.2805T + 0.0049T^2;\\
(n_i - 1)/\rho_i = 1.0923 - 0.00126T;\\
m_{g1\kappa} = 0.194 + 0.00126T;\\
m_{g2\kappa} = 0.499 + 0.01T + 2.365\times10^{-4}T^2;\\
\kappa_m/\rho_m = 0.00926 + 2.872\times10^{-4}T;\\
\kappa_b/\rho_b = 0.467 + 0.00724T;\\
K_t/\rho_t = 2.783 + 0.0689T;\\
\kappa_i/\rho_i = 0.32 + 0.00516T.
\end{gathered} \tag{5}$$

Formulas (1)–(5) represent a refractive model of the complex dielectric permittivity of thawed and frozen organic soil at 6.9 GHz. To calculate the complex dielectric permittivity of organic soil, we only need to specify the gravimetric moisture content, dry soil density, and temperature. It should be noted that in the measurements (Mironov et al., 2010), the soil sample was frozen at −7°C. This delay in freezing temperature was because the soil sample was placed in a closed coaxial container. For this reason, dielectric model (1)–(5) can be used to describe frozen and thawed soils only in the temperature ranges of $-30°C \le T \le -7°C$ and $-7°C \le T \le 25°C$, respectively. However, in nature, the freezing temperature of the soil is determined by many factors. Depending on the content of salts, acids, and capillary structure of the soil, the freezing point can vary in the range of negative temperatures ranging from tenths of degrees Celsius to several degrees. We performed an additional cycle of measurements in which freezing of the studied soil was noted at −1°C. This was achieved by inducing the initial crystallization nuclei at −7°C, followed by a subsequent freezing process at −1°C.

In the next section, using these data, it will be shown that formulas (5) and the model as a whole can be used for frozen soil in the temperature range of $-30°C \le T \le -1°C$ for the case when the soil was frozen at −1°C.

SIMULATION RESULTS

The complex dielectric permittivity (CDP) of the studied organic soil was calculated. Model calculations of the soil's CDP depending on the volumetric moisture content were compared with the measured values of the real, $\varepsilon' = n^2 - \kappa^2$, and imaginary, $\varepsilon'' = 2n\kappa$, parts of the CDP for thawed (Fig. 2a) and frozen (Fig. 2b) soil. In this case, Fig. 2 shows the measured values that were used to derive formulas (5) and (6) representing the dielectric model.

Figure 2 shows that the model describes very well both the real and imaginary parts of the complex dielectric permittivity of the soil depending on its moisture content in the temperature ranges of $-30°C \le T \le -7°C$ in the case of frozen soil and $0°C \le T \le 25°C$ in the case of thawed soil.

To verify the proposed dielectric model in an extended temperature range of $-30°C \le T \le -1°C$, additional measurements of soil samples with the various moisture content at a soil freezing temperature of −1°C were performed. This was achieved by inducing initial crystallization nuclei at −7°C and then freezing the sample at −1°C. Table 2 shows the gravimetric

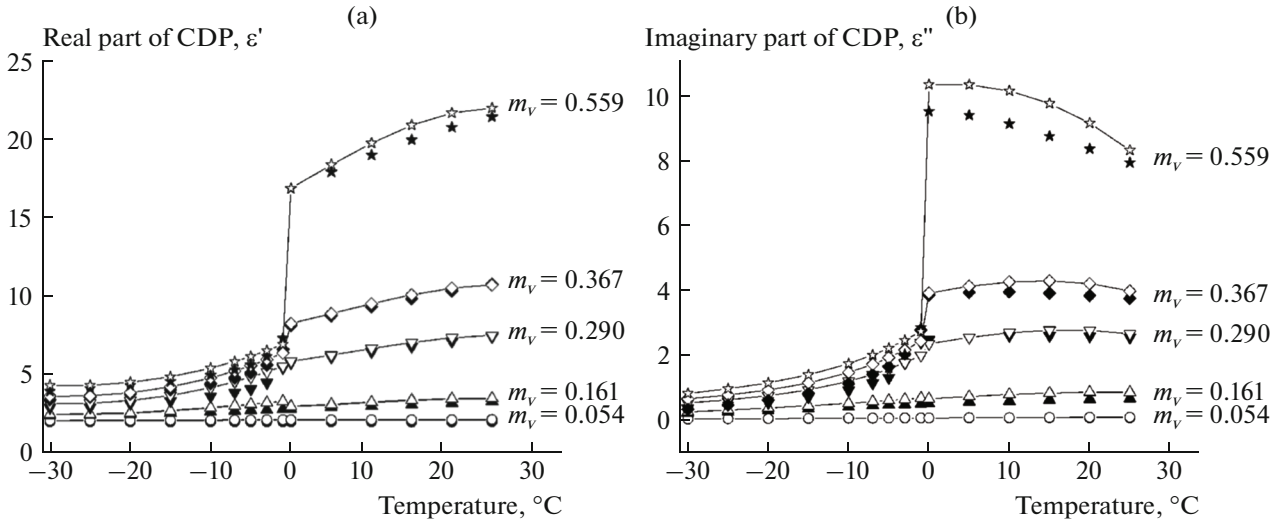

Fig. 3. Dependences of the measured (filled symbols) and calculated (lines + empty symbols) complex dielectric permittivity of soil on temperature at various values of volumetric moisture m_v (values shown on the graph): (a) real part of CDP, (b) imaginary part of CDP.

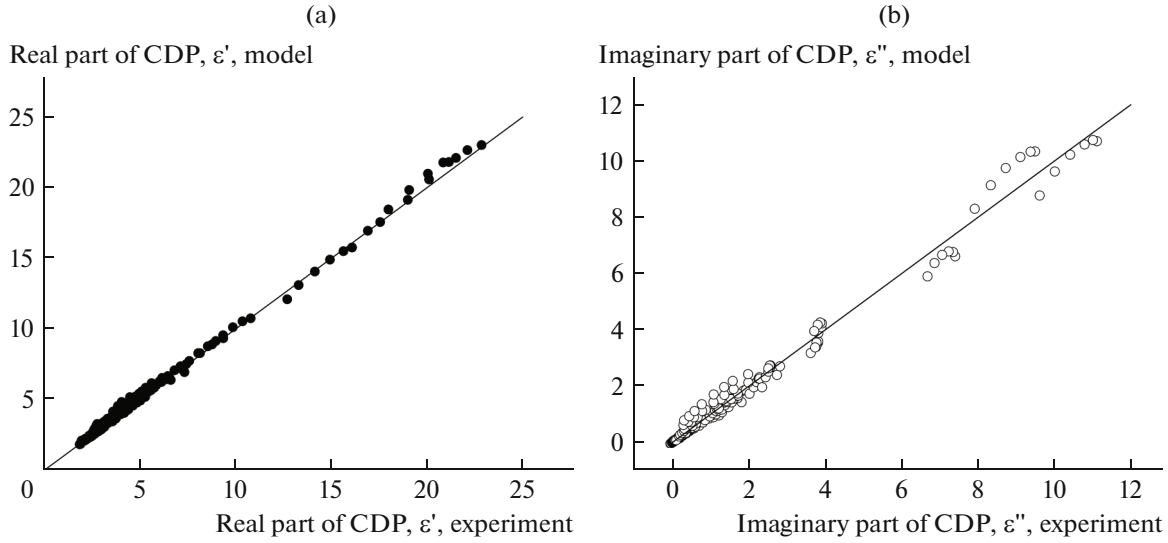

Fig. 4. Dependence of the values of the complex dielectric permittivity of the soil calculated by the model on the measured CDP values of the soil: (a) for the real part of CDP, (b) for the imaginary part of CDP. The solid line is the bisector.

moisture m_g, dry bulk density ρ_d, and volumetric moisture m_v of the soil samples used in the additional measurements.

The dielectric measurement data thus obtained can be considered independent when testing the developed dielectric model (2)–(5), including the temperature range of $-7°C \le T \le -1°C$.

Figure 3 shows the dependences of the measured and calculated complex soil permittivity on temperature at various moisture levels (0.054, 0.161, 0.290, 0.367, and 0.599 cm^3/cm^3). As can be seen in Fig. 3, the values of the complex and imaginary parts of the soil permittivity that are measured and calculated using the created dielectric model are in satisfactory agreement with each other, including the temperature range of $-7°C \le T \le -1°C$. To estimate the modeling error, both the measurement results used to build the model and the results of independent measurements at a soil freezing temperature of $-1°C$ at all humidity and temperature values were used. Figure 4 shows the cal-

Table 2. Dry soil density ρ_d, gravimetric m_g and volumetric m_v moisture observed in an additional experiment with the freezing point close to zero

m_g	0.086	0.114	0.299	0.516	0.602	0.992
ρ_d	0.633	0.611	0.538	0.541	0.570	0.531
m_v	0.054	0.070	0.161	0.290	0.367	0.559

culated values of the ε' real and ε'' imaginary parts of the CDP, depending on the measured values. The model errors calculated as the standard deviations of the calculated values from the measured values (RMSE) were 0.20 and 0.22 for the real and imaginary parts of theCDP. In this case, the values of the coefficients of determination (R^2) were 0.999 and 0.995, respectively.

CONCLUSIONS

Based on the laboratory dielectric measurements, a single-frequency dielectric model of organic tundra soil was developed. The model allows calculating the complex dielectric permittivity of thawed and frozen soil depending on moisture at 6.9 GHz in the temperature ranges of $-30°C \le T \le -1°C$ and $0°C \le T \le 25°C$. The refractive dielectric model of the mixture was used to describe the dependence of the complex refractive index of the soil on the moisture content. The soil is considered as a five-component system consisting of a mineral-organic component, air, and three types of water (bound, transitional, and free). The parameters of the refractive model are the complex refractive indices and the values of the maximal allowable content of various types of water in the soil that are determined based on the results of measurements of the complex refractive index of soil samples.

As a result of comparing the values of the complex dielectric permittivity calculated using the model with the measured values, RMSE estimates were obtained for the real (RMSE $\varepsilon' = 0.2$) and imaginary (RMSE $\varepsilon'' = 0.22$) parts of the complex permittivity at values of the determination coefficient of 0.999 and 0.995, respectively. This error is comparable to the errors in the initial measurements of the complex dielectric permittivity of wet soil. In the future, we intend to create a dielectric model of Arctic soils with various fractions of organic and mineral components.

CONFLICT OF INTEREST

The authors declare that they have no conflict of interest.

REFERENCES

De Roo, R.D., England, A.W., Gu, H., Pham, H., and Elsaadi, H., Groundbased radiobrightness observations of the active layer growth on the north slope near Toolik Lake, Alaska, Proc. IEEE IGARSS. Denver, Colo., July 31–Aug. 4, 2006, pp. 2708–2711. http://suzaku.eorc.jaxa.jp/GCOM-W/index.html.

Kerr, Ya.H., Waldteufel, P., Richaume, P., Wigneron, J.-P., Ferrazzoli, P., Mahmoodi, A., Al Bitar, A., Cabot, F., Gruhier, C., Juglea, S.E., Leroux, D., Mialon, A., and Delwart, S., The SMOS soil moisture retrieval algorithm, *IEEE Trans. Geosci. Remote Sens.*, 2012, vol. 50, no. 5, pp. 1384–1400.

Mironov, V.L. and Fomin, S.V., Temperature and mineralogy dependable model for microwave dielectric spectra of moist soils, *PIERS Proc. August 18–21, 2009*, Moscow, 2009, pp. 938–942.

Mironov, V.L. and Savin, I.V., Temperature dependence of dielectric permeability of the tundra soil under conditions of water freezing in soil capillaries, *Izv. Vyssh. Uchebn. Zaved., Fiz.*, 2010, vol. 53, no. 9, pp. 241–246.

Mironov, V.L., De Roo, R.D., and Savin, I.V., Temperature-dependable microwave dielectric model for an Arctic soil, *IEEE Trans. Geosci. Remote Sens.*, 2010, vol. 48, no. 6, pp. 2544–2556.

Mladenova, I.E., Jackson, T.J., Njoku, E., Bindlish, R., Chan, S., Cosh, M.H., Holme, T.R.H., De Jeud, R.A.M., Jones, L., Kimball, J., Paloscia, S., and Santi, E., Remote monitoring of soil moisture using passive microwave-based techniques: Theoretical basis and overview of selected algorithms for AMSR-E, *Remote Sens. Environ.*, 2014, vol. 144, pp. 197–213.

Pumpanen, J. and IIvesniemi, H., Calibration of time domain reflectometry for forest humus soil layers, *Boreal Environ. Res.*, 2005, vol. 10, pp. 589–595.

Rozanov, B.G., *Geneticheskaya morfologiya pochv* (Genetic Morphology of Soils), Moscow: MGU, 1975.

Scierucha, W., Accuracy of soil moisture measurement by TDR technique, *Int. Agrophys.*, 2000, vol. 14, pp. 417–426.

Topp, G.C., Davis, J.L., and Annan, A.P., Electromagnetic determination of soil water content: Measurements in coaxial transmission lines, *Water Resour. Res.*, 1980, vol. 16, no. 3, pp. 574–582.

Translated by A. Ivanov